PROCEDURE OF EVALUATION OF TRANSPORTATION LAGS IN WELD FORMATION ACS

V.V. DOLINENKO, V.A. KOLYADA, T.G. SKUBA and **E.V. SHAPOVALOV**
E.O. Paton Electric Welding Institute, NASU, Kiev, Ukraine

A method is suggested for determination of transportation lags in feedback circuit of automatic system for control of weld reinforcement formation process in MAG welding. Mechanism of emergence of two different transportation lags, i.e. formation of weld reinforcement height and width, which are revealed by measurements of its geometric parameters by a laser TV-sensor, has been investigated. To estimate the transportation lags, it is suggested using the regression formulae derived on the basis of computational experimental results. A mathematical model of the weld pool developed for conditions of item heating with the movable normal-circular heat source has been used as an object of the computational experiments.

Keywords: *arc welding, welded joints, weld shape, ACS, transportation lag, laser-TV sensor*

The problem of closed-loop control of formation of the weld in arc welding has for a long time attracted the attention of specialists in the field of welding process automaton. One of the main challenges in solving this problem is realization of feedback by parameters determining the weld shape. In [1] it is proposed to perform closed-loop control of the process of weld formation using weld pool observation with a special sensor, the functioning of which is based on the method of two-colour pyrometry. Such an approach allows obtaining only indirect assessments of weld parameters, which can essentially differ from actual values. Of great interest is the method, proposed in [2], which suggests using direct measurement of geometrical parameters of weld reinforcement with a laser-TV sensor (LTVS). The fact that the presence of several transportation lags between LTVS and weld pool sections is not taken into account can be regarded as one of the disadvantages of the known schematics of closed-loop control of weld formation. Therefore, control stability can deteriorate at the change of the welding mode parameters.

This work proposes a procedure of assessment of transportation lags for automatic control systems (ACS) of MAG welding, in which the feedback is provided using LTVS [3].

It is known from the theory of welding processes that bead width and height correspond to pool solidification front in its middle and tail parts [4]. Figure 1 shows the schematic of formation of two transportation lags in ACS using LTVS (separately for measurement of height g and width e of weld reinforcement). The dashed line outlines the contour of an imaginary weld pool at the moment of time, when the projection of the electrode axis was in point O. Weld shape corresponds to the direction of welding from left to right. Point A indicates the extreme point of the solidification front of the weld pool tail part. Its coordinate along the abscissa axis determines the start of formation of the height of weld reinforcement. Points B and B' indicate the points of the weld pool solidification front in its middle part. Their coordinates along the abscissa axis determine the start of formation of weld reinforcement width. Distance between the electrode (welding torch axis) and LTVS light trace L_{TV} determines the base value of transportation lag at the change of bead parameters. Distance between point A (B) and point O along the abscissa axis is equal to $L_g(L_e)$. Thus, the values of portions of transportation lags of following width ΔL_e and height ΔL_g of weld bead are calculated as follows: $\Delta L_e = L_{TV} - L_e$, $\Delta L_g = L_{TV} - L_g$. Hence, the formulas for calculation of time parameters of transportation lags become:

$$\tau_g = \frac{L_{TV} - L_g}{v_w}; \quad \tau_e = \frac{L_{TV} - L_e}{v_w}, \qquad (1)$$

where τ_e, τ_g are the time parameters of transportation lags of measurements of bead width and height, respectively, s; v_w is the welding speed, cm/s.

It is seen from the Figure that in order to determine the value of transportation lags between the weld pool and LTVS light trace, it is necessary to know coordinates of points A, B, B' relative to the current coordinate of the projection of electrode axis O. However,

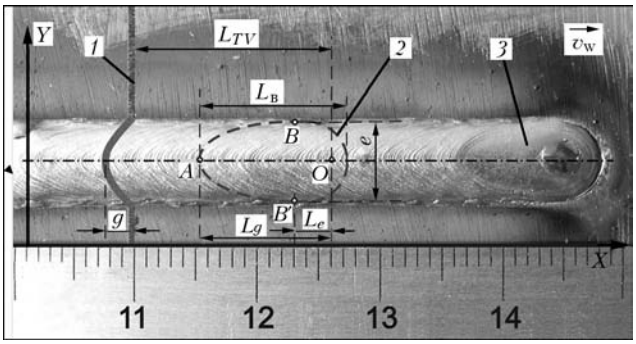

Figure 1. Schematic of emergence of transportation lags between the weld pool and LTVS in MAG welding: *1* — LTVS light trace; *2* — imaginary contour of weld pool; *3* — surface of solidified weld pool

© V.V. DOLINENKO, V.A. KOLYADA, T.G. SKUBA and E.V. SHAPOVALOV, 2010

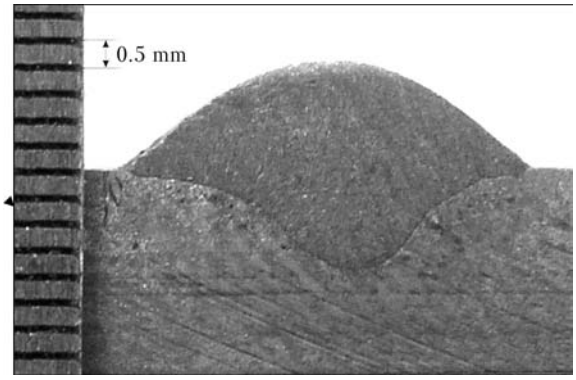

Figure 2. Weld macrosection (U_a = 19 V; I_w = 160 A; v_w = = 0.75 cm/s)

for a symmetrical bead shape, abscissas of points B and B' are equal, so that calculation is required only for points A and B.

In order to solve this problem, a mathematical model was synthesized, which allows calculation of weld pool geometrical parameters based on heat transfer in the welded items. Equation describing the process of heat propagation in a semi-infinite body at its heating by a moving normal-circular source [5], has the following form:

$$T(x, y, z, t) = \frac{2q}{c\gamma(4\pi a)^{3/2}} \exp\left(-\frac{v_w x}{2a}\right) \int_0^t \frac{dt''}{\sqrt{t''(t_0 + t'')}} \times \times \exp\left[-\frac{z^2}{4at''} - \frac{r^2}{4a(t_0 + t'')} - \frac{v_w^2}{2a}(t_0 + t'')\right], \quad (2)$$

where $r^2 = x^2 + y^2$, cm^2; x, y, z are the coordinates of the current calculation point of the temperature field, cm; $a = \lambda/c\gamma$ is the thermal diffusivity, J/m^2; $c\gamma$ is the bulk heat content, J/(m^3·K); $q = 0.24\eta U_a I_w$ is the effective heat power, J/m; U_a, I_w are the average values of welding voltage and current; $t_0 = 1/(4ak_t)$ is the duration of propagation of a fictitious source, s; k_t is the coefficient of heat concentration of the arc, cm^{-2}; t is the time interval of the action of a continuous mobile heat source, s; $t'' = t - t'$, s; t' is the auxiliary moment of time, in which the source applied heat in the initial section of its motion, s.

Numerical solution was fulfilled with sampling increment of 0.01 cm. Ignoring the processes of mass transfer into the weld pool, can be regarded as one of the disadvantages of such a solution.

Welding experiments were performed to precise the values of the main energy parameters of the thermal model. Reverse polarity welding was performed in shielding gas (Ar + 15 % CO_2) in the downhand position. Carbon steel plates 0.8 mm thick (butt welding) were welded with Sv-08G2S electrode wire of 0.12 cm diameter. Rated parameters of welding mode were as follows: I_w = 160 A, U_a = 19 V, v_w = 7.5 cm/s. Figure 2. shows a macrosection of the weld bead used to verify the adequacy of the thermal model. Results of welding experiments were used to more precisely determine the values of thermal model parameters: effective efficiency of welding η = 0.75 and coefficient of concentration of the arc thermal action k_t = 8.3 cm^{-2}. Other parameters of the thermal model have the following values: a = 0.0718 J/m^2, $c\gamma$ = 0.975 J/(m^3·K).

The computational experiment was performed in keeping with the full factorial plan of second order experiments [6]. The following variables were considered: U_a = 17–21 V, I_w = 145–175 A and v_w = 0.5–1.0 cm/s. Calculation of such weld pool parameters, as width e of weld pool, maximum penetration depth h, weld pool length L_p, distances L_e and L_g, was performed. The following ranges of parameters variation were obtained: h = 0.15–0.25 cm, e = 0.70–0.91 cm, L_p = 0.98–1.22 cm, which corresponds to the welding experiment. Results of the computational experiment are given in the Table. Normalized factors x_1, x_2 and x_3 correspond to factorial variables U_a, I_w and v_w.

Matrix of computational experiment and calculation results

#	x_1	x_2	x_3	U_a, V	I_w, A	v_w, cm/s	L_g, cm	L_e, cm
1	0	0	0	19.0	160	0.75	1.08	0.59
2	−1	−1	−1	17.8	151	0.60	0.95	0.48
3	−1	−1	1	17.8	151	0.90	1.04	0.57
4	−1	1	−1	17.8	169	0.60	1.02	0.47
5	−1	1	1	17.8	169	0.90	1.11	0.68
6	1	−1	−1	20.2	151	0.60	1.04	0.51
7	1	−1	1	20.2	151	0.90	1.13	0.59
8	1	1	−1	20.2	169	0.60	1.13	0.48
9	1	1	1	20.2	169	0.90	1.22	0.68
10	−1.68	0	0	17.0	160	0.75	0.99	0.59
11	0	−1.68	0	19.0	145	0.75	1.01	0.60
12	0	0	−1.68	19.0	160	0.50	0.99	0.50
13	1.68	0	0	21.0	160	0.75	1.16	0.51
14	0	1.68	0	19.0	175	0.75	1.16	0.63
15	0	0	1.68	19.0	160	1.00	1.14	0.65

The following regression formulas are obtained:

$$L_g = -0.69 + 0.041U_a + 0.0048I_w + 0.3v_w \text{ (cm)}; \quad (3)$$

$$L_e = 0.08 + 0.004U_a + 0.0016I_w + 0.4v_w \text{ (cm)}. \quad (4)$$

Mean root square error of approximation for regression model (3), (4) does not exceed 5 %.

According to the proposed procedure, a priori information about value L_{TV} and ranges of variation of welding variables I_w, U_a and v_w is used to calculate the ranges of variation of distances L_e and L_g, and then formula (1) is used to calculate minimum and maximum evaluations of transportation lags τ_e and τ_g.

Let us consider as an example a practical case with L_{TV} = 7.5 cm. Comparing maximum changes of transportation lags for a constant and varying welding speed at variation of welding mode in the following range: U_a = 17–21 V and I_w = 145–175 A. In the first case, for v_w = 0.75 cm/s calculation yields the range

of variation of τ_e = 9.0–9.1 s (relative change is equal to 1 %) and τ_g = 8.4–8.8 s (5 %). In the second case for the range of variation v_w = 0.5–1.0 cm/s changes of transportation lags are as follows: τ_e = 6.7–13.8 s (relative change of 78 %) and τ_g = 6.2–13.3 s (83 %). Thus, in the second case, the model of control object is a non-stationary dynamic system which requires more sophisticated control algorithms.

The proposed procedure of calculation of transportation lags in weld reinforcement formation ACS with feedback allows correct selection of time parameters and type of automatic regulator.

1. Zhang, H., Pan, J., Lao, B. (1999) The real-time measurement of welding temperature field and closed-loop control of isotherm width. *Sci. in China Press*, 21(**2**), 129–135.
2. Doumanidis, C., Kwak, Y.-M. (2002) Multivariable adaptive control of the bead profile geometry in gas metal arc welding with thermal scanning. Intern. *J. Pressure Vessels and Piping*, **79**, 251–262.
3. Kiselevsky, F.N., Shapovalov, E.V., Kolyada, V.A. (2006) System of laser following of weld reinforcement bead. *The Paton Welding J.*, **1**, 42–44.
4. Erokhin, A.A. (1973) *Fundamentals of fusion welding. Physico-chemical principles*. Moscow: Mashinostroenie.
5. Rykalin, N.N., Uglov, A.A. (1951) *Calculations of thermal processes in welding*. Moscow: Mashgiz.
6. Johnson, I., Lion, F. (1981) *Statistics and experiment planning in engineering and science: methods of experiment planning*. Moscow: Mir.

THESIS FOR A SCIENTIFIC DEGREE

E.O. Paton Electric Welding Institute of the NAS of Ukraine

On December 10, 2009, **A.V. Yarovitsyn** (PWI) defended his Candidate of Sciences Thesis on subject «Microplasma Powder Cladding of Heat-Resistant Nickel Alloy with 45–65 % γ-phase Content».

The thesis is dedicated to investigation of the energy, thermal and technological peculiarities of microplasma powder cladding with the aim of development of a commercial technology for repair of blades from heat-resistant nickel alloys.

The thesis substantiates requirements to a welding heat source for microplasma powder cladding. It shows that a combination of low specific heat inputs of 100–650 W, low heat power density in an equivalent heat spot equal to 150–1500 W/cm^2 and low speed of the microplasma arc provides slow cooling of the base metal in the brittle temperature intervals at a rate of 3–10 °C/s. In this case the strain growth rate does not exceed the critical values, and initiation of hot cracks is hardly possible in the most dangerous zone of the base metal. The microplasma arc stability at a current of 2–35 A with portioned feed of a powder to the arc column, depending on the level of constriction of the arc by plasma nozzles, was investigated. It was determined that destabilization of the microplasma arc at currents of less than 22–25 A is caused by the influence on the arc by the carrier gas dosing pulses moving in a flow-through gas-powder system at a speed of up to 60 m/s. Proportion of a carrier gas dosing pulse speed of 5–15 m/s and specific plasma gas flow rate of 2–4 m/s was experimentally found to provide the stable arc.

It was established, based on experimental calorimetry data, that at currents of 5–35 A the effective methods for control of the heat power density in the microplasma arc heating spot include the effective heat power of the arc equal to 100–600 W, constriction of the arc due to changes in diameters of the plasmatron nozzle channels and shielding gas types (Ar or a mixture of Ar + 10 % H_2), and concentrated powder feed. In microplasma powder cladding the heat power density in the equivalent heat spot is 100–250 W/cm^2, which is 3–8 times lower in comparison with the arc for the low-current TIG process. Such heat characteristics of the microplasma arc provide a more uniform metal cooling and, combined with its speed of about 1 m/h, efficiently limit the strain rate.

The thesis determines that in microplasma powder cladding of heat-resistant nickel alloys the oxygen content of the deposited metal varies in a range of 0.0068–0.0220 %, and the nitrogen content — in a range of 0.0026–0.0080 %. It was experimentally proved that it is necessary and efficient to limit the oxygen content in the deposited metal of heat-resistant nickel alloys to 0.006–0.009 % by providing the following process parameters: plasmatron-to-workpiece distance of 2.5–5.0 mm, using powders with a low oxygen content, and using a mixture of Ar + 10 % H_2 as a shielding gas.

The thesis established the feasibility of microplasma powder cladding at currents of 5–35 A on a narrow substrate, and at currents of 17–35 A on a wide substrate.

The technology was developed for repair of ends of band flanges of blades from heat-resistant nickel alloy JS32-VI for aircraft engine D18T. The technology is based on application of one-layer cladding at currents of 8–20 A using additive powder of JS32 alloy. The feasibility was proved of repair of polycrystalline blades by microplasma powder cladding using additives with a composition identical to that of the base metal of JS6U-VI alloy, as well as less heat-resistant additives with a specified level of properties for alloys JS6K-VI and ChS70-VI.